

Temperature Dependence of the Impact Ionization Coefficients in AlAsSb Lattice Matched to InP

Xiao Jin , Shiyu Xie , Baolai Liang, Xin Yi, Harry Lewis , Leh W. Lim , Yifan Liu, Beng Koon Ng, Diana L. Huffaker, *Fellow, IEEE*, Chee Hing Tan , *Senior Member, IEEE*, Duu Sheng Ong , and John P. R. David , *Fellow, IEEE*

Abstract—The temperature dependence of the ionization coefficients of AlAsSb has been determined from 210 K to 335 K by measuring the avalanche multiplication in a series of three p^+i-n^+ and two n^+i-p^+ diodes. Both electron and hole ionization coefficients reduce at approximately the same rate as the temperature increases but much less so than in InAlAs or InP. This results in a significantly smaller breakdown voltage variation with temperature of 13 mV/K in a 1.55 μm thick p^+i-n^+ structure and a calculated 15.58 mV/K for a 10 Gb/s InGaAs/AlAsSb separate absorption and multiplication avalanche photodiode (SAM-APD). Monte-Carlo modelling suggests that the primary reason for this reduced temperature dependence is the increased alloy scattering in the Sb containing alloy, reducing the impact of variation in phonon scattering rate with temperature.

Index Terms—Avalanche breakdown, avalanche photodiode (APD), impact ionization, AlAsSb, InP, InAlAs temperature dependence, ionization coefficient, Monte Carlo modelling.

Manuscript received May 19, 2021; revised July 11, 2021; accepted July 20, 2021. Date of publication July 26, 2021; date of current version September 6, 2021. The work of Chee Hing Tan and John P.R. David was supported in part by Engineering and Physical Science Research Council (EPSRC) under Grant EP/N020715/1. The work of Diana L. Huffaker was supported in part by the Sêr Cymru National Research Network in Advanced Engineering and Materials. The work of Shiyu Xie was supported in part by the European Regional Development Fund through the Welsh Government. The work of Harry Lewis was supported in part by EPSRC studentship under Grant EP/R513313/1. (*Corresponding author: Xiao Jin.*)

Xiao Jin, Harry Lewis, Leh W. Lim, Yifan Liu, Chee Hing Tan, and John P. R. David are with the Electronic and Electrical Engineering Department, University of Sheffield, Sir Frederick Mappin Building, Mappin Street Sheffield S1 3JD, United Kingdom (e-mail: xjin4@sheffield.ac.uk; hlewis2@sheffield.ac.uk; lwlim1@sheffield.ac.uk; yfliu1@sheffield.ac.uk; c.h.tan@sheffield.ac.uk; j.p.david@sheffield.ac.uk).

Shiyu Xie is with the School of Physics and Astronomy, Cardiff University, Cardiff CF24 3AA, U.K. (e-mail: xies1@cardiff.ac.uk).

Baolai Liang is with the California Nano Systems Institute, University of California-Los Angeles, Los Angeles, CA 90095 USA (e-mail: bliang@cnsi.ucla.edu).

Xin Yi is with the Electronic and Electrical Engineering Department, University of Sheffield, Sir Frederick Mappin Building, Mappin Street Sheffield S1 3JD, United Kingdom. He is now with the School of Engineering and Physical Sciences, Heriot-Watt University, Edinburgh EH14 4AS, U.K. (e-mail: xin.yi@hw.ac.uk).

Beng Koon Ng is with the School of Electrical & Electronic Engineering, Nanyang Technological University, Singapore 639798, Singapore (e-mail: ebkng@ntu.edu.sg).

Diana L. Huffaker is with the School of Physics and Astronomy, Cardiff University, Cardiff CF24 3AA, U.K., and also with the California Nano Systems Institute, University of California-Los Angeles, Los Angeles, CA 90095 USA (e-mail: huffaker@ee.ucla.edu).

Duu Sheng Ong is with the Faculty of Engineering, Multimedia University, 63100 Cyberjaya, Selangor, Malaysia (e-mail: dsong@mmu.edu.my).

Color versions of one or more figures in this article are available at <https://doi.org/10.1109/JSTQE.2021.3099912>.

Digital Object Identifier 10.1109/JSTQE.2021.3099912

I. INTRODUCTION

AVALANCHE photodiodes (APDs) are widely used in optical detection systems as they can provide higher sensitivity and a larger signal to noise ratio than p-i-n diodes due to the internal gain that is provided by avalanche multiplication. This avalanche multiplication is a result of the impact ionization process that electrons and holes undergo at high electric fields, which can be highly temperature dependent. For impact ionization to occur, carriers need to gain the ionization threshold energy by traversing the high field multiplication region. This threshold energy depends on the bandgap energy (E_g) [1], which is only weakly dependent on temperature [2]. Prior to an impact ionization event, carriers travelling in an electric-field gain and lose energy due to various scattering processes [3]. Of these, phonon scattering is the most temperature dependent process and can make the overall avalanche multiplication factor highly temperature sensitive. To ensure that the linear mode avalanche gain, and hence the sensitivity, of an APD receiver module, or the breakdown voltage and overbias in a Geiger mode APD, does not change with temperature, an active variable bias circuit is sometimes required to modify the reverse bias voltage across the device as the temperature changes [4]. Alternatively, the temperature must be regulated by an embedded thermoelectric cooler (TEC) and temperature sensor for the purpose of temperature stabilization [5]. Both add extra complexity and cost to the receiver modules unless the APD is made of a material which has a weak temperature dependent ionization process and small temperature coefficient of breakdown voltage,

$$C_{bd} = \Delta V_{bd} / \Delta T,$$

where ΔV_{bd} is the change in breakdown voltage and ΔT is the difference in temperature. These C_{bd} values are material dependent and can be significant in silicon APDs (1.1 V/°C) [6] and in InGaAs APDs (0.1 V/°C) [7]. As carriers undergoing impact ionization in a thicker avalanching structure will encounter more phonons than in a thinner structure, they will undergo a larger change in V_{bd} with temperature, so it is necessary to ensure that the widths of the high field regions are similar when comparing different material systems.

Recently, there has been considerable interest in Sb containing III-V alloy systems for use as the multiplication region in APDs. These materials show significantly larger electron to hole impact ionization coefficient (α to β) ratios [8]–[10]

compared to silicon, InP or even InAlAs, so are attractive for low noise APDs [11]. Xie *et al.* demonstrated a small C_{bd} of 0.95 - 1.47 mV/K for 80 - 230 nm thick AlAsSb lattice matched to InP [12]. Some of the reasons for using very thin avalanche regions are to utilize the ‘dead-space’ (the minimum distance carriers need to travel to be in equilibrium with the electric-field), to reduce the ionization excess noise [13]. Thin structures also provide a higher gain-bandwidth product for a given α/β ratio [14], and benefit from having a smaller C_{bd} . However the appearance of Sb containing alloys with very large α/β ratios means that we can now achieve both very low noise and very high gain-bandwidth product (GBP) operation with fairly thick avalanching structures. While the C_{bd} of AlInAsSb alloy with thick avalanching structures (0.89 μm) has been investigated [15], [16], no such study exists for AlAsSb. Unlike AlInAsSb, which is lattice matched to GaSb, AlAsSb is lattice matched to InP and InGaAs, offering the prospect for very high sensitivity telecommunications APDs operating at very high bit rates [17]. In this work, we look at the avalanche multiplication characteristics in five AlAsSb p-i-n and two n-i-p structures that cover avalanche region widths of 80 nm to 1.55 μm over a temperature range of 210K to 335K. From these, we extracted the temperature dependent ionization coefficients over a wide electric field range of 220kV/cm to 1250kV/cm and compared them to InP and InAlAs structures. We also highlight some of the challenges in undertaking these measurements accurately in materials that have a large α/β ratio and a relatively small C_{bd} . Finally, we undertake Monte Carlo modelling to explain the mechanism behind the reduced temperature dependence seen in AlAsSb.

II. LAYER DETAILS

The AlAsSb p^+-i-n^+ and n^+-i-p^+ structures P1-P3 and N1-N2 were grown by a digital alloy growth technique as described previously [9]. P4 and P5 are two thin structures for which the change in breakdown voltage with temperature has been previously reported [12], [18]. To enable direct comparisons to be made in the same measurement set-up, three further structures were investigated; two InAlAs structures (P6, N3) and one InP structure (P7). All structures grown are homojunctions with heavily doped top cladding layers that are >200 nm thick and undoped intrinsic regions. The depletion region widths were determined by fitting the experimental capacitance-voltage (C-V) to an electric field solver based on Poisson’s equation and are detailed in Table I. By using standard photolithography and wet chemical etching circular mesa diodes were fabricated with diameters from 50 μm to 420 μm .

III. METHODS

AlAsSb has an indirect bandgap of $\sim 1.55\text{eV}$ at room temperature and therefore should have a low bulk dark current. However, due to the high surface leakage current of the unpassivated mesa diodes (especially at high temperatures), a phase sensitive detection technique was used to extract the photocurrent multiplication measurement with modulated 405 nm laser light for AlAsSb and 532 nm for InAlAs and InP. These wavelengths

TABLE I
A SUMMARY OF DETAILS OF THE LAYERS USED IN THIS WORK

| Layer details | Material | Layer structure | Nominal i -region thickness (μm) | CV fitted i -region thickness (μm) | i -region doping level ($\times 10^{15}\text{cm}^{-3}$) |
|---------------|----------|-----------------|---|---|---|
| P1 | AlAsSb | PIN | 1.5 | 1.56 | 5 |
| N1 | AlAsSb | NIP | 1.5 | 1.58 | 7 |
| P2 | AlAsSb | PIN | 0.6 | 0.66 | 8 |
| N2 | AlAsSb | NIP | 0.6 | 0.66 | 8 |
| P3 | AlAsSb | PIN | 1 | 1.15 | 10 |
| P4 | AlAsSb | PIN | 0.25 | 0.23 | 1 |
| P5 | AlAsSb | PIN | 0.1 | 0.08 | 1 |
| P6 | InAlAs | PIN | 1.01 | 1.01 | 3 |
| N3 | InAlAs | NIP | 0.5 | 0.51 | 5 |
| P7 | InP | PIN | 0.55 | 0.51 | 1 |

have $>99\%$ absorption in the top doped cladding layers and so ensure pure electron (in p^+-i-n^+) and hole (in n^+-i-p^+) initiated multiplication (M_e and M_h respectively). Photocurrent measurements as a function of reverse bias voltage were repeated at different optical powers and on several devices to ensure their repeatability. The real multiplication is determined by applying a bias-dependent collection efficiency correction to the measured photocurrent versus voltage characteristic to account for the movement of the depletion edge at the p^+ (n^+) – i region in the p^+-i-n^+ (n^+-i-p^+) structures respectively [19]. This enables the multiplication to be determined to an accuracy of 5% or better. To measure small values of C_{bd} we need to know the actual junction temperature, and this is determined using the forward voltage drop at a current of 1 μA as an indication of the actual junction temperature. This shows a linear relationship as shown in Fig. 1(a) for P3. The temperature dependent forward I-V also enables us to determine an activation energy for the material (Fig. 1(b)) at 0V, which at $\sim 0.8\text{eV}$ is very close to $E_g/2$. When temperature dependent photomultiplication measurements were undertaken, as detailed in the subsequent section, in a low temperature cryostat or on a heater stage, forward I-V measurements were also undertaken to confirm the temperature of the device under test.

IV. TEMPERATURE DEPENDENT AVALANCHE MULTIPLICATION CHARACTERISTICS

In most semiconductors where the temperature dependence of ionization coefficients have been investigated such as silicon [20], GaAs [21], InP [22] and AlGaAs [23], both α and β decrease at approximately the same rate with increasing temperature. However, the behavior in a digitally grown InAlAs alloy has been reported to be different, with α decreasing and β increasing with increasing temperature [24]. Extracting the values of α and β as a function of temperature requires us to have photomultiplication measurements on p^+-i-n^+ and n^+-i-p^+ structures, preferably with different avalanching widths to cover a wide electric field range.

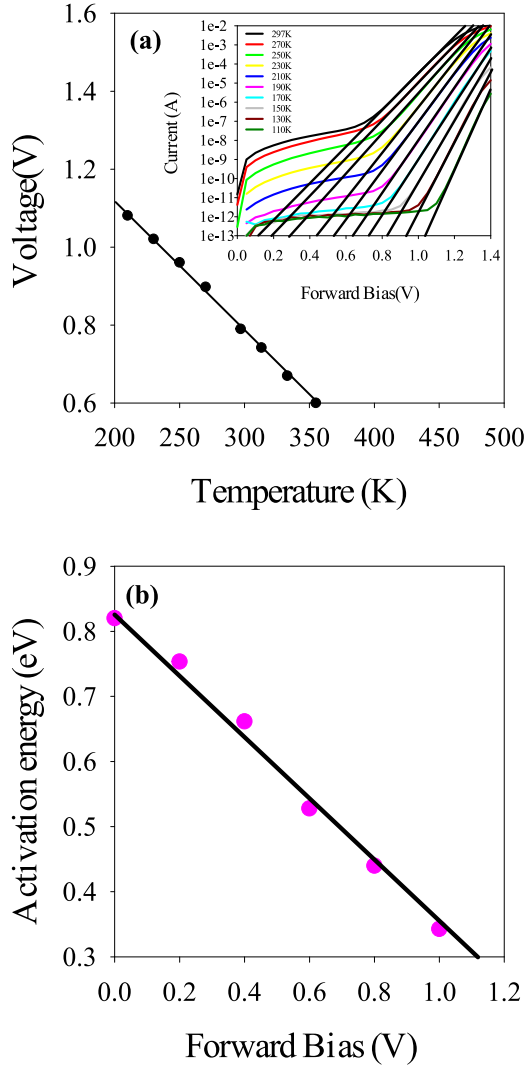


Fig. 1. (a) Forward voltage drops across a $420\mu\text{m}$ diameter P3 device at $1\mu\text{A}$ over a wide temperature range used to calibrate the junction temperature. Inset shows the forward I-V characteristics at different temperatures. (b) Activation energy calculated from the temperature dependence forward bias voltages.

Measurements of M_e and M_h were undertaken between 210K and 335K at 30-40K intervals. Fig. 2(a) shows only the M_e taken at 210K, 295K and 335K on the three thick AlAsSb p^+-i-n^+ structures (P1, P2, P3), with the others omitted for clarity. The change in the multiplication with temperature is small in even the thickest AlAsSb structure (P1). This change is smaller in the $1.15\mu\text{m}$ structure (P3) and continues to decrease in the $0.66\mu\text{m}$ structure (P2). Measurements on the two thinnest structures (P4, P5) show extremely small changes between 210K and room temperature in agreement with earlier results [12]. The results on the two AlAsSb n^+-i-p^+ structures (N1, N2) show that M_h behaves in a similar manner with changing temperature to M_e . Fig. 2(b) shows the multiplication from P1 and N1 plotted as $M-1$ on a log scale to accentuate the temperature dependence at very low values of multiplication. Also shown for comparison is the $M-1$ for the $1.01\mu\text{m}$ thick InAlAs (P6) and the $0.55\mu\text{m}$ thick InP p^+-i-n^+ structures (P7).

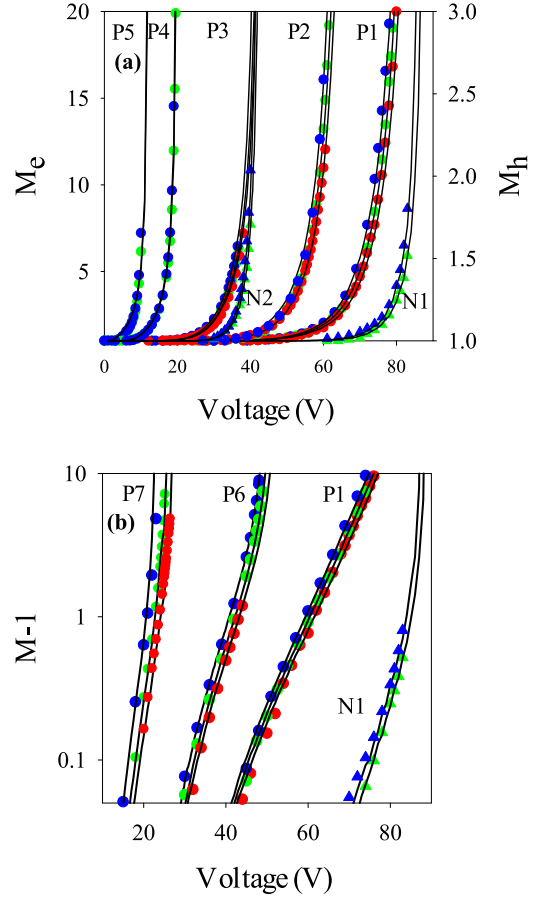


Fig. 2. (a) Temperature dependent multiplication in different thickness AlAsSb p-i-n and n-i-p diodes. (b) Temperature dependent $M-1$ for the $\sim 1.55\mu\text{m}$ thick AlAsSb p^+-i-n^+ and n^+-i-p^+ structures (P1, N1), $1.01\mu\text{m}$ InAlAs (P6) and $0.55\mu\text{m}$ thick InP (P7). The blue, green and red symbols represent measurements at 210K; 295K; and 335K respectively. Solid lines are modelled results using the parameterized ionization coefficients.

Values of M_h could only be obtained up to ~ 2 in the AlAsSb n^+-i-p^+ samples, due to the fact that very high electric-fields are necessary to measure any hole multiplication in this material system [9]. For $M < 1.05$, the ionization process is primarily due to the injected carrier type unlike at higher values of M when feedback results in both electrons and holes contributing to the multiplication. Comparing P1 and N1 in Fig. 2(b) therefore suggests that both α and β decrease with increasing temperature in AlAsSb and by approximately similar amounts. The results also show that despite the InAlAs (P6) and InP (P7) structures being thinner, they show larger changes with temperature.

Using the multiplication data shown in Figs. 2(a) and 2(b), the ionization coefficients were extracted by solving the ionization integral across the multiplication region given by [25]:

$$M(x) = \frac{\exp[-\int_0^x (\alpha(x') - \beta(x')) dx']}{1 - \int_0^W \alpha(x') \exp[-\int_0^{x'} (\alpha(x'') - \beta(x'')) dx''] dx'}$$

where $M(x_0)$ is the multiplication due to the injection of an electron-hole pair at position x_0 , and W is the width of the high field region. Uncertainties in W are largely due to the C-V measurements and dielectric constant value assumed, giving rise to a 3% uncertainty in the exact electric field.

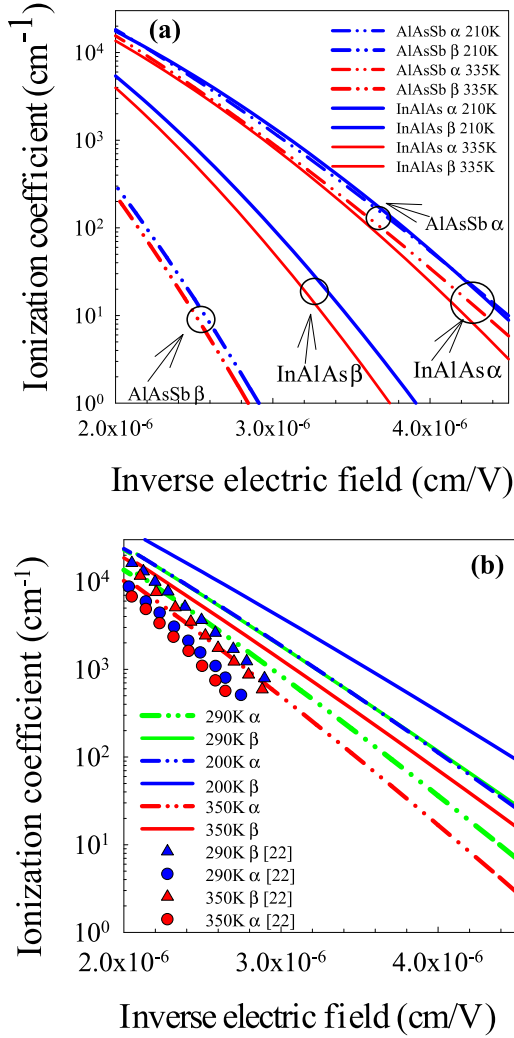


Fig. 3. (a) Ionization coefficient variation with temperature for both AlAsSb and InAlAs from 210K to 335K. Solids lines are AlAsSb and dots are InAlAs. (b) Ionization coefficient variation with temperature for InP from 200K to 350K.

The variation in the electric field across the depletion region due to the background doping was accounted for in a numerical model when extracting α and β , and these are shown in Figs. 3(a) and (b) for temperatures from 210K to 335K. While both α and β decrease with increasing temperature in AlAsSb, the change is very small and only significant at the lower electric fields. A similar analysis was undertaken on the multiplication from the InAlAs (P6, N3) and InP (P7) structures, supplemented with data from ref [26]. Fig. 3(a) shows that between 210K to 335K and for an ionization coefficient of 100 cm⁻¹, the electric-field has to increase by $\sim 2.4\%$ for α and 3.4% for β in AlAsSb. For InAlAs, however, the increase is much larger, at 4.8% for α and 5.7% for β . The change in InP is significantly larger over the same temperature range (not shown in Fig. 3(b)), with the electric fields increasing by 11.6% for α and 11.4% for β . The results from Taguchi *et al.* [22] are shown in Fig. 3(b) for comparison and a similar temperature dependence is observed as the temperature increases from 290K to 350K. The temperature dependent ionization coefficients for AlAsSb, InAlAs and InP are parameterized into the following equations [25], which can

be used to estimate the multiplication and breakdown voltage as a function of temperature. These temperature dependent ionization coefficients assume that the carriers are only dependent on their local electric field and do not take any account of ‘dead-space’ effects [27] or their history [28]. While this will overestimate the low values of multiplication in very thin avalanching structures [29], it will not affect the accuracy of the multiplication in most thick APDs. This is demonstrated by the modelled results in Figs. 2(a) and (b), which agree well with experimental data.

For AlAsSb:

- For 220 KV/cm $\leq E \leq 500$ KV/cm and

$$\alpha(E, T) = 5.70 \times 10^5 \exp \left[- \left(\frac{3.49 \times 10^2 \times T + 1.10 \times 10^6}{E} \right)^{1.43} \right] \text{cm}^{-1} \quad (2a)$$

- For 500 KV/cm $< E \leq 1250$ KV/cm

$$\alpha(E, T) = 3.90 \times 10^5 \exp \left[- \left(\frac{2.73 \times 10^2 \times T + 1.18 \times 10^6}{E} \right)^{1.25} \right] \text{cm}^{-1} \quad (2b)$$

- For 360 KV/cm $\leq E \leq 1250$ KV/cm

$$\beta(E, T) = 3.20 \times 10^5 \exp \left[- \left(\frac{2.39 \times 10^2 \times T + 1.63 \times 10^6}{E} \right)^{1.60} \right] \text{cm}^{-1} \quad (2c)$$

For InAlAs:

- For 220 KV/cm $\leq E \leq 980$ KV/cm and

$$\alpha(E, T) = 2.20 \times 10^5 \exp \left[- \left(\frac{3.97 \times 10^2 \times T + 7.76 \times 10^5}{E} \right)^{1.71} \right] \text{cm}^{-1} \quad (2d)$$

$$\beta(E, T) = 2.95 \times 10^5 \exp \left[- \left(\frac{3.89 \times 10^2 \times T + 1.04 \times 10^6}{E} \right)^{1.71} \right] \text{cm}^{-1} \quad (2e)$$

For InP:

- For 180 KV/cm $\leq E \leq 480$ KV/cm

$$\beta(E, T) = 1.41 \times 10^6 \exp \left[- \left(\frac{1.67 \times 10^3 \times T + 1.22 \times 10^6}{E} \right)^{1.23} \right] \text{cm}^{-1} \quad (2f)$$

$$\beta(E, T) = 2.11 \times 10^6 \exp \left[- \left(\frac{1.68 \times 10^3 \times T + 1.32 \times 10^6}{E} \right)^{1.15} \right] \text{cm}^{-1} \quad (2g)$$

- For 480 KV/cm $\leq E \leq 750$ KV/cm

$$\alpha(E, T) = 1.41 \times 10^6 \exp \left[- \left(\frac{2.01 \times 10^3 \times T + 1.30 \times 10^6}{E} \right)^{1.15} \right] \text{cm}^{-1} \quad (2h)$$

$$\beta(E, T) = 2.20 \times 10^6 \exp \left[- \left(\frac{2.37 \times 10^3 \times T + 1.53 \times 10^6}{E} \right)^{1.01} \right] \text{cm}^{-1} \quad (2i)$$

Determination of the breakdown voltage at different temperatures is often done by plotting the inverse of the multiplication ($1/M$) and extrapolating it to zero [30]. This $1/M$ becomes increasingly inaccurate as a predictor of V_{bd} as the α/β ratio increases, as shown in Fig. 4. The larger the α/β ratio, as in the thicker AlAsSb structures, the larger the multiplication needs to be, to accurately predict V_{bd} . Even values of M_e up to 40 ($1/M_e = 0.025$) for P1 will not enable an accurate extrapolation of

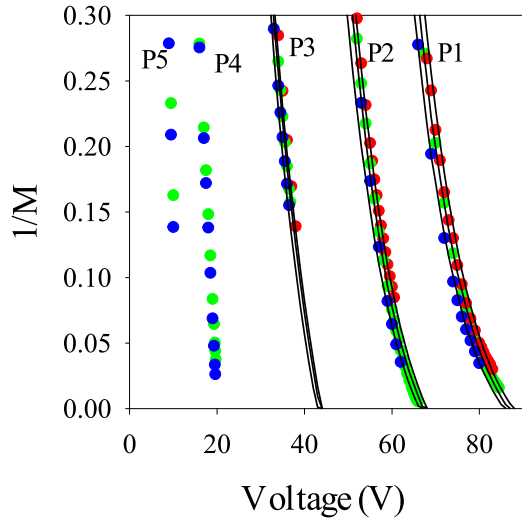


Fig. 4. Determination of V_{bd} from $1/M$ showing an increasingly non-linear behaviour when the α/β ratio is large. The blue (210K), green (295K), and red (335) symbols refer to the experimental data taken on the five AlAsSb p^+-i-n^+ structures. No high temperature measurements were done on the two thinnest p^+-i-n^+ structures (P4, P5). The solid black lines are calculations using equations 2a-2c.

the $1/M_e$ line. Using empirical expressions like those suggested by Miller [31] to predict M and estimate V_{bd} appear to work well only for materials with α/β ratios close to unity. Accurate predictions of V_{bd} should instead rely on calculating the M_e from the ionization coefficients as shown by the solid lines in Fig. 4. Changes in voltage required for $M_e = 6$ (or larger) measured experimentally, however, seem to agree closely with those calculated at breakdown (to within 3%) and so this can be used to provide us with accurate estimates of C_{bd} .

The C_{bd} of different thickness p^+-i-n^+ or n^+-i-p^+ diodes for different semiconductors obtained in this study are shown in Fig. 5. Data for the different thicknesses of InP and InAlAs structures taken from [32] are shown as the green and blue symbols respectively. Results from P7, P6, and N3 (shown as symbols) agree well with this data. The C_{bd} decreases with decreasing avalanche thickness because carriers experience fewer phonon collisions prior to impact ionization at the higher electric fields [20],[33]. The C_{bd} in AlAsSb is however significantly lower than those of InAlAs and InP of similar thicknesses. The results for P1-P3 are in good agreement with the previously published results on P4 and P5. The relationship between the i-region thickness and C_{bd} for different materials can be parameterized as:

$$C_{bd} = P \times W_m \text{ mVK}^{-1} \quad (3a)$$

Where P is the C_{bd} gradient for different materials and W_m is the i-region thickness in μm . P is 8.5, 16.5, 25, 43 mV/K/ μm for AlAsSb, InAlAs, Si, and InP respectively and is shown by the solid black lines in Fig. 5. Here we assume that the C_{bd} is equal to zero when there is no depletion region. This expression holds true when the electric-field is constant across the avalanche region width as in perfect p^+-i-n^+ or n^+-i-p^+ structures. In very

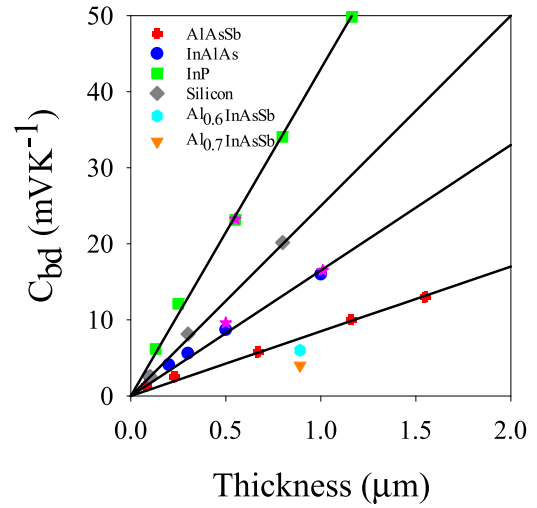


Fig. 5. Comparison of C_{bd} in AlAsSb (red symbols) of this work with the reported data for other semiconductors including InP [32], InAlAs[32], Si[20], AlInAsSb [16]. (*) are the measurements on InP and InAlAs done respectively in this study. Black lines are the estimated values of P for the different materials.

thin structures, the cladding layer depletion needs to be taken into consideration to get agreement with P . From Fig. 5, for a given thickness of $0.6\mu\text{m}$, the C_{bd} for InP, Si, InAlAs and AlAsSb are 25.3mV/K, 15.5 mV/K, 10.5mV/K and 5.14 mV/K respectively. Interestingly, the $\text{Al}_{0.7}\text{In}_{0.3}\text{As}_{0.3}\text{Sb}_{0.7}$ quaternary alloy grown lattice matched to GaSb has been reported recently as having an even lower C_{bd} than AlAsSb (shown in Fig. 5).

Telecommunication wavelength APDs utilize a thick InGaAs absorption region at a low electric field and a high field multiplication region in a SAM-APD structure. It is straightforward to show that the C_{bd} of a SAM-APD depends on the C_{bd} of the multiplication region width $C_{bd}(W_m)$ and the total depletion of the device, as:

$$C_{bd} (\text{SAM APD}) = C_{bd} (W_m) \times \frac{W_{depletion}}{W_m} \text{ mVK}^{-1} \quad (3b)$$

where $W_{depletion}$ is the total depletion width of the SAM APD and W_m is the multiplication region thickness [32].

By substituting equation 3a into 3b, the C_{bd} expression for a SAM APD can be given as:

$$C_{bd} (\text{SAM APD}) = P \times (W_{abs} + W_{cg} + W_m) \text{ mVK}^{-1} \quad (3c)$$

Where W_{abs} is the absorber thickness and W_{cg} is the thickness of the charge/grading layers.

A 10Gb/s SAM APD using a $1.1\mu\text{m}$ InGaAs absorber requires a $0.2\mu\text{m}$ InAlAs multiplication region with a V_{bd} of around 32V [34], and this would have an estimated C_{bd} of 28.3mV/K. Replacing the $0.2\mu\text{m}$ InAlAs multiplication layer with $0.6\mu\text{m}$ of AlAsSb would still enable operation at 10Gb/s with a larger V_{bd} , but would have a better sensitivity (due to the larger α/β ratio) [17] and a much lower C_{bd} of 15.58mV/K.

V. DISCUSSION

The weak temperature dependence of α and β in ternary semiconductors can be attributed to the presence of alloy scattering, which is considered insensitive to temperature changes [35]. The effect of alloy scattering on the temperature dependence of α in InGaAs [36] and on the breakdown field in AlGaAs ($x = 0.6$) [33] has been shown using analytical-band Monte Carlo (MC) models. These simulations showed that the alloy scattering contributes significantly to the overall scattering rate, reducing the relative importance of phonon scatterings in these ternary alloys. In this work, we employ a conventional analytical-band MC model [37] to demonstrate the effect of alloy scattering on the temperature dependence of β , in AlAsSb and InAlAs semiconductors. The scattering mechanisms considered in this MC model are acoustic, polar optical, non-polar optical, intra- and inter-band phonon scattering processes and alloy scattering for hole transport in the first three valence bands (the heavy hole, light hole and spin-split off bands). This MC model is used to reproduce the field dependence of β in AlAsSb and InAlAs at a temperature of 335K, as shown in Fig. 6. The alloy disorder potential used is 0.9eV for AlAsSb and 0.6eV for InAlAs, comparable to the values calculated by Ong *et al.* [38] based on the electronegativity difference of Phillips [39]. Changing the temperature to 210K while keeping the other parameters essentially identical shows that the model produces results that are in good agreement with β from the experimental measurements for both AlAsSb and InAlAs at this temperature. In order to demonstrate the role of alloy scattering on the weak temperature dependence of β in AlAsSb, we repeated the simulations but this time reducing the alloy potential in AlAsSb to that of InAlAs, i.e., 0.6 eV, while increasing the phonon scattering rates to reproduce the β at 335K (grey dashed line in Fig. 6). The simulations now show a much more significant increase in β at 210K as shown in Fig. 6 by the solid grey line. This is due to holes experiencing less alloy scattering while the temperature sensitive phonon scatterings have a relatively more significant effect. Therefore, this suggests that the temperature dependence of ionization coefficients in any alloy semiconductor is not just determined by the phonon (or total scattering rates) but by the ratio of phonon scatterings and alloy scattering rates in that material. Sb has a large mass, so the phonon energy of Sb alloys is likely to be smaller, leading to possibly a higher number of phonons. However, this may not be as important as the relative increase in the proportion of scattering events that are due to alloy scattering. Therefore, a material with a large alloy potential like AlAsSb can exhibit a weak temperature dependence of ionization coefficients given that alloy scattering plays a more dominant role in the carrier transport before impact ionization. The even lower C_{bd} seen in $\text{Al}_{0.7}\text{In}_{0.3}\text{As}_{0.3}\text{Sb}_{0.7}$ [16] may be due to the fact that it has more Sb than AlAsSb, or because it is a quaternary alloy.

VI. CONCLUSION

Measurements of the avalanche multiplication in a range of AlAsSb p-i-n and n-i-p diodes from 210K to 335K show that α and β both decrease as the temperature increases and at similar

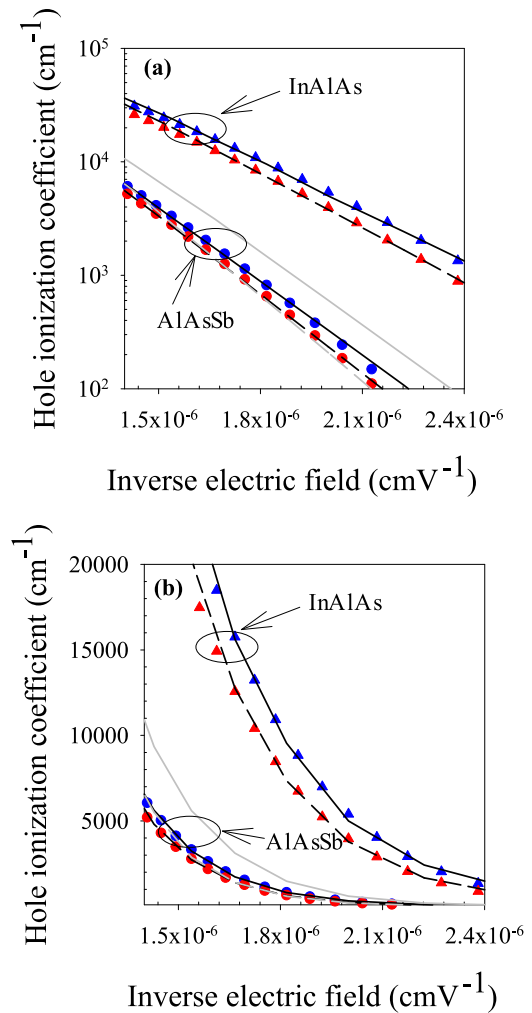


Fig. 6. (a) Analytical-band MC model for temperature dependence of the β in AlAsSb and InAlAs Symbols are data from Fig. 3 and lines (solid lines (210K) and dashed lines (335K)) are MC simulation results. (b) Shows the same data but in a linear plot.

rates. The change in α and β with temperature decreases as the electric field increases. AlAsSb also shows a significantly lower breakdown voltage variation with temperature than equivalent thickness InAlAs and InP structures. Monte Carlo modelling suggests that the larger alloy potential of AlAsSb is primarily responsible for this reduced temperature sensitivity. The weaker temperature dependence of AlAsSb means that thicker avalanching regions can be used in SAM-APD structures, and these are still likely to be better than using InP or InAlAs multiplication regions.

REFERENCES

- [1] K. Yeom, J. M. Hinckley, and J. Singh, "Theoretical study on threshold energy and impact ionization coefficient for electrons in $\text{Si}_{1-x}\text{Ge}_x$," *Appl. Phys. Lett.*, vol. 64, no. 22, pp. 2985–2987, 1994, doi: [10.1063/1.111379](https://doi.org/10.1063/1.111379).
- [2] P. Varshni, "Temperature dependence of the energy gap in semiconductors," *Physica*, vol. 34, pp. 149–154, 1967.
- [3] M. V. Fischetti, "Monte carlo simulation of transport in technologically significant semiconductors of the diamond and zinc-blende structures-part I: Homogeneous transport," *IEEE Trans. Electron Devices*, vol. 38, no. 3, pp. 634–649, Mar. 1991.

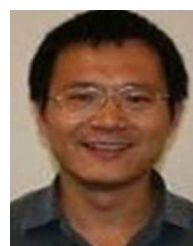
- [4] S. Deng, A. P. Morrison, and J. Hayes, "A bias and control circuit for gain stabilization in avalanche photodiodes," in *Proc. IET Ir. Signals Syst. Conf.*, 2013, pp. 37–37, doi: [10.1049/ic.2012.0187](https://doi.org/10.1049/ic.2012.0187).
- [5] Princetonlightwave, "PAR series - High sensitivity APD front end receiver modules," PAR-M-1550TO, 2016, Accessed: May 2021.
- [6] HAMAMATSU, "High-sensitivity Si APD for detection of light with a wavelength of 266 nm," Cat. No. KAPD1081E02, Jun. 2020, Accessed: May 2021.
- [7] HAMAMATSU, "High-speed response," Cat. No. KAPD1018E06, Jul. 2018, Accessed: May 2021.
- [8] Y. Yuan *et al.*, "AlInAsSb impact ionization coefficients," *IEEE Photon. Technol. Lett.*, vol. 31, no. 4, pp. 315–318, Feb. 2019, doi: [10.1109/LPT.2019.2894114](https://doi.org/10.1109/LPT.2019.2894114).
- [9] X. Yi *et al.*, "Demonstration of large ionization coefficient ratio in AlAs_{0.56}Sb_{0.44} lattice matched to InP," *Sci. Rep.*, vol. 8, no. 1, pp. 8–13, 2018, doi: [10.1038/s41598-018-27507-w](https://doi.org/10.1038/s41598-018-27507-w).
- [10] S. Lee *et al.*, "Low noise Al_{0.85}Ga_{0.15}As_{0.56}Sb_{0.44} avalanche photodiodes on InP substrates," *Appl. Phys. Lett.*, vol. 118, no. 8, pp. 0–5, 2021, doi: [10.1063/5.0035571](https://doi.org/10.1063/5.0035571).
- [11] R. J. McIntyre, "Multiplication noise in uniform avalanche diodes," *IEEE Trans. Electron Devices*, vol. ED-13, no. 1, pp. 164–168, Jan. 1966.
- [12] S. Xie and C. H. Tan, "AlAsSb avalanche photodiodes with a Sub-mV/K temperature coefficient of breakdown voltage," *IEEE J. Quantum Electron.*, vol. 47, no. 11, pp. 1391–1395, Nov. 2011, doi: [10.1109/JQE.2011.2165051](https://doi.org/10.1109/JQE.2011.2165051).
- [13] K. F. Li *et al.*, "Avalanche multiplication noise characteristics in thin GaAs p⁺-i-n⁺ diodes," *IEEE Trans. Electron Devices*, vol. 45, no. 10, pp. 2102–2107, Oct. 1998.
- [14] R. B. Emmons, "Avalanche-Photodiode frequency response," *J. Appl. Phys.*, vol. 38, no. 9, pp. 3705–3714, Aug. 1967, doi: [10.1063/1.1710199](https://doi.org/10.1063/1.1710199).
- [15] A. H. Jones *et al.*, "Al_xIn_{1-x}As_ySb_{1-y} photodiodes with low avalanche breakdown temperature dependence," *Opt. Exp.*, vol. 25, no. 20, 2017, Art. no. 24340, doi: [10.1364/oe.25.024340](https://doi.org/10.1364/oe.25.024340).
- [16] M. Ren *et al.*, "Operation stability study of AlInAsSb avalanche photodiodes," in *Proc. IEEE Photon. Conf.*, 2017, pp. 159–160.
- [17] X. Yi *et al.*, "Extremely low excess noise and high sensitivity AlAs_{0.56}Sb_{0.44} avalanche photodiodes," *Nat. Photon.*, vol. 13, no. 10, pp. 683–686, 2019, doi: [10.1038/s41566-019-0477-4](https://doi.org/10.1038/s41566-019-0477-4).
- [18] I. C. Sandall, S. Xie, J. Xie, and C. H. Tan, "High temperature and wavelength dependence of avalanche gain of AlAsSb avalanche photodiodes," *Opt. Lett.*, vol. 36, no. 21, 2011, Art. no. 4287, doi: [10.1364/ol.36.004287](https://doi.org/10.1364/ol.36.004287).
- [19] M. H. Woods, W. C. Johnson, and M. A. Lampert, "Use of a schottky barrier to measure impact ionization coefficients in semiconductors," *Solid State Electron.*, vol. 16, no. 3, pp. 381–394, 1973, doi: [10.1016/0038-1101\(73\)90013-0](https://doi.org/10.1016/0038-1101(73)90013-0).
- [20] D. J. Massey, J. P. R. David, and G. J. Rees, "Temperature dependence of impact ionization in submicrometer silicon devices," *IEEE Trans. Electron Devices*, vol. 53, no. 9, pp. 2328–2334, Sep. 2006.
- [21] C. Groves, R. Ghin, J. P. R. David, and G. J. Rees, "Temperature dependence of impact ionization in GaAs," *IEEE Trans. Electron Devices*, vol. 53, no. 9, pp. 2328–2334, Oct. 2006.
- [22] K. Taguchi, T. Torikai, Y. Sugimoto, K. Makita, and H. Ishihara, "Temperature dependence of impact ionization coefficients in InP," *J. Appl. Phys.*, vol. 59, no. 2, pp. 476–481, Jan. 1986, doi: [10.1063/1.336655](https://doi.org/10.1063/1.336655).
- [23] C. Groves, C. N. Harrison, J. P. R. David, and G. J. Rees, "Temperature dependence of breakdown voltage in AlGa_{1-x}As," *J. Appl. Phys.*, vol. 96, no. 9, pp. 5017–5019, 2004, doi: [10.1063/1.1803944](https://doi.org/10.1063/1.1803944).
- [24] Y. Yuan *et al.*, "Comparison of different period digital alloy," *J. Lightw. Technol.*, vol. 37, no. 14, pp. 3647–3654, 2019, doi: [10.1109/JLT.2019.2918676](https://doi.org/10.1109/JLT.2019.2918676).
- [25] A. G. Chynoweth, "Ionization rates for electrons and holes in silicon," *Phys. Rev.*, vol. 109, no. 5, pp. 1537–1540, Mar. 1958, doi: [10.1103/PhysRev.109.1537](https://doi.org/10.1103/PhysRev.109.1537).
- [26] L. J. J. Tan, "Telecommunication wavelength InP based avalanche photodiodes," Ph.D dissertation, Dept. Electron. Elect. Eng., Univ. Sheffield, Sheffield, U.K., Apr. 2008, Accessed: May 10, 2021.
- [27] M. M. Hayat, W. L. Sargeant, and B. E. A. Saleh, "Effect of dead space on gain and noise in Si and GaAs avalanche photodiodes," *IEEE J. Quantum Electron.*, vol. 28, no. 5, pp. 1360–1365, May 1992.
- [28] R. J. McIntyre, "A new look at impact ionization-part I: A theory of gain, noise, breakdown probability, and frequency response," *IEEE Trans. Electron Devices*, vol. 46, no. 8, pp. 1623–1631, Aug. 1999.
- [29] S. A. Plimmer *et al.*, "The effect of an electric-field gradient on avalanche noise," *Appl. Phys. Lett.*, vol. 75, no. 19, pp. 2963–2965, 1999, doi: [10.1063/1.125202](https://doi.org/10.1063/1.125202).
- [30] X. Zhou, S. Zhang, J. P. R. David, J. S. Ng, and C. H. Tan, "Avalanche breakdown characteristics of Al_{1-x}Ga_xAs_{0.56}Sb_{0.44} quaternary alloys," *IEEE Photon. Technol. Lett.*, vol. 28, no. 22, pp. 2495–2498, Nov. 2016.
- [31] S. L. Miller, "Ionization rates for holes and electrons in silicon," *Phys. Rev.*, vol. 105, no. 4, pp. 1246–1249, Feb. 1957, doi: [10.1103/PhysRev.105.1246](https://doi.org/10.1103/PhysRev.105.1246).
- [32] L. J. J. Tan *et al.*, "Temperature dependence of avalanche breakdown in InP and InAlAs," *IEEE J. Quantum Electron.*, vol. 46, no. 8, pp. 1153–1157, Aug. 2010.
- [33] F. Ma *et al.*, "Low-temperature breakdown properties of Al_xGa_{1-x}As avalanche photodiodes," *Appl. Phys. Lett.*, vol. 81, no. 10, pp. 1908–1910, 2002, doi: [10.1063/1.1506012](https://doi.org/10.1063/1.1506012).
- [34] A. E. Shimura and E. Yagyu, "High sensitivity 2.5/10 gbps InAlAs avalanche photodiodes," Mitsubishi Elect., Adv. 127, Sep. 17–29, 2009.
- [35] D. K. Ferry, "Alloy scattering in ternary III-V compounds," *Phys. Rev.*, vol. 17, no. 2, pp. 1–2, 1978.
- [36] K. Y. Choo and D. S. Ong, "Positive and negative temperature dependences of electron-impact ionization in In_{0.53}Ga_{0.47}As," *J. Appl. Phys.*, vol. 98, no. 2, 2005, doi: [10.1063/1.1993755](https://doi.org/10.1063/1.1993755).
- [37] D. S. Ong *et al.*, "A monte carlo investigation of multiplication noise in thin p⁺-i-n⁺ GaAs avalanche photodiodes," *IEEE Trans. Electron Devices*, vol. 45, no. 8, pp. 1804–1810, Aug. 1998.
- [38] J. S. L. Ong, J. S. Ng, A. B. Krysa, and J. P. R. David, "Temperature dependence of avalanche multiplication and breakdown voltage in Al_{0.52}In_{0.48}P," *J. Appl. Phys.*, vol. 115, no. 6, pp. 0–6, 2014, doi: [10.1063/1.4865743](https://doi.org/10.1063/1.4865743).
- [39] J. C. Phillips, "Ionicity of the chemical bond in crystals," *Rev. Mod. Phys.*, vol. 42, no. 3, pp. 317–356, 1970, doi: [10.1103/RevModPhys.42.317](https://doi.org/10.1103/RevModPhys.42.317).



His research interests include the characterization of III-V semiconductor material and devices, especially that AlAsSb/AlGaAsSb material systems.



by the European Regional Development Fund through Welsh government Ser Cymru Fellowship Program, leading and developing a novel antimony-based solid-state material system and sensors. Since March 2021, she has been a Research Director at Advanced Microsemi working on optoelectronic devices.



Xiao Jin received the B.Eng. degree in 2018 in electronic electrical engineering from The University of Sheffield, Sheffield, U.K., where he is currently working toward the Ph.D. degree with Semiconductor Group. The aim of his Ph.D. research is to develop ADPs capable of operating at very high speeds and high sensitivity for next generation telecommunication networks. He is studying the impact ionization process via different modeling techniques and look experimentally at the ionization coefficient in different semiconductor materials and device structures.

Shiyu Xie received the B.S. degree from the Huazhong University of Science and Technology, Wuhan, China, in 2007 and the Ph.D. degree in electronic and electrical engineering from The University of Sheffield, Sheffield, U.K., in 2012. From 2012 to 2014, she was with Huawei Corporation, as a Research Engineer. From 2014 to 2016, she was a Postdoctoral Fellow with The University of Sheffield and Cardiff University, Cardiff, U.K., respectively. From January 2017 to February 2021, she was a Research Fellow with Cardiff University sponsored

Baolai Liang received the Ph.D. degree in microelectronics-photonics from the University of Arkansas, Fayetteville, AR, USA. He is currently the Director of the Integrated Nanomaterials Laboratory, California NanoSystems Institute, University of California, Los Angeles, Los Angeles, CA, USA. His current research interests include molecular beam epitaxy growth and optical characterizations of low-dimensional III-V semiconductor materials for optoelectronics device application.



Xin Yi received the B.Eng. and Ph.D. degrees in electronic and electrical engineering from The University of Sheffield, Sheffield, U.K., in 2015 and 2020, respectively. He is currently a Research Associate with Heriot-Watt University, Edinburgh, U.K. His research interests include ultrahigh-speed avalanche photodiode, single-photon avalanche diodes, and LiDA.



Harry Lewis received the M.Eng. degree in 2018 from the University of Sheffield, Sheffield, U.K., where he is currently working toward the Ph.D. degree with the Impact Ionization Group. His research interests include impact ionisation in III-V semiconductors, with a focus on the measurement and characterisation of excess noise and the development of low-noise APDs, and low-noise analogue circuitry.



Leh W Lim received the B.Eng. degree in 2016 in electronic and electrical engineering from the University of Sheffield, Sheffield, U.K., where he is currently working toward the Ph.D. degree study on III-V avalanche photodiode materials, specializing in fabrication and characterization. His current research interests are in design and modeling of silicon photonic devices.



Yifan Liu received the B.Eng. degree in electronic and electrical engineering from the Southeast University, Nanjing, China, in 2018. She is currently working toward the Ph.D. degree with the Impact Ionization Group, University of Sheffield, Sheffield, U.K. Her research interests include characterization of III-V semiconductor materials and avalanche photodiode.



Beng Koon Ng received the B.Eng. and M.Eng. degrees in electrical and electronic engineering from Nanyang Technological University, Singapore, in 1997 and 2000, respectively, and the Ph.D. degree in 2003 from the Department of Electronic and Electrical Engineering, University of Sheffield, Sheffield, U.K., where he investigated the impact ionization process in wide bandgap semiconductors for applications in telecommunications and solar/visible-blind UV avalanche photodiodes (APDs). He is currently a Faculty Member of the School of Electrical and Electronic Engineering, Nanyang Technological University. In addition to APD research, he is also investigating the use of Biophotonics imaging techniques for cancer detection. He is a Member of the IEEE Electron Devices Society and the IEEE Lasers and Electro-Optics Society.



Diana L. Huffaker (Fellow, IEEE) was the Welsh Government Sêr Cymru Chair in advanced materials and engineering. She was the Science Director of the Institute for Compound Semiconductors (ICS) with considerable experience in managing large, multi-institutional programmers supported by the U.S. National Science Foundation and Department of Defense. Since August 2020, she has been the Chair of the Electrical Engineering Department, University of Texas at Arlington, Arlington, TX, USA. She is a pioneer in MBE growth of III-Sb bulk and quantum dot materials and recently demonstrated growth of Sb material using the DA technique. Her research interests include novel III-As-Sb epitaxial methods, fabrication, and high-performance detectors.



Chee Hing Tan (Senior Member, IEEE) received the B.Eng. and Ph.D. degrees in electronic engineering from the Department of Electronic and Electrical Engineering, University of Sheffield, Sheffield, U.K., in 1998 and 2002, respectively. He is currently a Professor of opto-electronic sensors and the Head of Department with the Department of Electronic and Electrical Engineering, University of Sheffield. He has extensive experience in the characterization and modeling of high-speed low-noise avalanche photodiodes and phototransistors. His current research interests include novel semiconductor materials, single-photon avalanche diodes, infrared photodiodes, X-ray detectors, and ultrahigh-speed avalanche photodiodes.



Duu Sheng Ong received the B.Sc. (Hons.) and M.Phil. degrees in physics from the University of Malaya, Malaysia, and the Ph.D. degree in electronics engineering from the University of Sheffield, Sheffield, U.K. He joined Multimedia University (MMU), Cyberjaya, Malaysia, in 1999 and obtained his Professorship with the Faculty of Engineering in 2009. He served MMU as the Director of Research Management Center, the Dean of the Institute for Postgraduate Studies and the Vice President (Academic) from 2008 to 2014. He is a Fellow of Institute of Physics Malaysia and a Principal Assessor of Malaysia Qualifications Agency. He holds the Chartered Physicist of Institute of Physics and Chartered Engineer of Engineering Council, U.K. He is a Humboldt Research Fellow and an alumnus of DAAD. Since 2014, he has been serving as a resource person for higher education leadership and quality assurance training programmes in southeast Asia. His current research interests include THz electronic devices, high field carrier transport in semiconductors, and modeling of novel low-dimensional materials.



John P. R. David (Fellow, IEEE) received the B.Eng. degree in electronic engineering and the Ph.D. degree from The University of Sheffield, Sheffield, U.K., in 1979 and 1983, respectively. From 1982 to 2001, he was a Postdoctoral Researcher with The University of Sheffield on the study of impact ionization coefficients and III-V materials characterization. From 2001 to 2002, he was a Senior Engineer with Bookham Technologies before returning to The University of Sheffield, as a Senior Lecturer. From 2002 to 2004, he was an IEEE LEOS Distinguished Lecturer, giving presentations on the topic of Low Noise Avalanche Photodiodes. He has authored or coauthored more than 350 journal articles and has a similar number of conference presentations in the areas of avalanche photodiodes, impact ionization, and III-Material characterization. He is a Fellow of IET.